Changes in Winter Temperature Extremes from Future Arctic Sea-Ice Loss and Ocean Warming

Y. T. Eunice Lo[1,2], Dann M. Mitchell[1,2], Peter A. G. Watson[1,2], and James A. Screen[3]

[1]School of Geographical Sciences, University of Bristol, Bristol, UK.

[2]Cabot Institute for the Environment, University of Bristol, Bristol, UK.

[3]College of Engineering, Mathematics and Physical Sciences, University of Exeter, Exeter, UK.

Corresponding author: Eunice Lo (eunice.lo@bristol.ac.uk)

Key Points:

- Less severe winter cold extremes in northern mid- and high-latitudes in response to future Arctic sea-ice loss
- Winter hot extremes increase in severity over high latitudes due to future Arctic sea-ice loss, but warm less than cold extremes
- In a majority of the latitudes, both cold and hot extremes warm more in response to future global SST change than due to sea-ice loss

Abstract

Observed rapid Arctic warming and sea-ice loss are likely to continue in the future, unless and after greenhouse gas emissions are reduced to net-zero. Here, we examine the possible effects of future sea-ice loss at 2°C global warming above pre-industrial levels on winter temperature extremes across the Northern Hemisphere, using coordinated experiments from the Polar Amplification Model Intercomparison Project. 1-in-20-year cold extremes are simulated to become less severe at high- and mid-latitudes in response to Arctic sea-ice loss. 1-in-20-year winter warm extremes become warmer at northern high latitudes due to sea-ice loss, but warm by less than cold extremes. We compare the response to sea-ice loss to that from global SST change also at 2°C global warming. SST change causes less severe cold extremes and more severe warm extremes globally. Except northern high latitudes, the response to SST change is of larger magnitude than that to Arctic sea-ice loss.

Plain Language Summary

The Arctic and neighbouring regions have rapidly warmed in recent decades and the sea ice has reduced. These changes will likely continue in future, unless greenhouse gas emissions from human activities are reduced to net-zero. Ongoing sea-ice loss can affect weather and climate across the Northern Hemisphere. We use climate models to study how extremely cold and hot temperatures in winter may change because of Arctic sea-ice loss. In a future world that is, on average, 2°C warmer than pre-industrial times, cold extremes will become less severe at high- and mid-latitudes because of Arctic sea-ice loss. Winter hot extremes also get warmer, but over fewer regions and not by as much as cold extremes. In the real world, changes in sea ice happen alongside changes in ocean temperatures. So, we also looked at the effect of ocean temperature changes in a 2°C warmer world on winter temperature extremes. Ocean warming will lead to warmer cold and hot extremes in the Northern Hemisphere. The effect from ocean warming is larger than that from Arctic sea-ice loss, meaning that even in the few places where sea-ice loss might cause cooling, it will be overwhelmed by warming due to the ocean temperature changes.

1 Introduction

Polar amplification, the phenomenon where near-surface air temperatures near the poles warm more than the global average in response to external radiative forcing, is a prominent feature of anthropogenic climate change. Since the late 20th century, the Arctic has warmed 3 to 4 times faster than the global mean (Rantanen et al., 2022), and September Arctic sea-ice extent has decreased by half (Francis & Wu, 2020). Arctic amplification is driven by local temperature, surface albedo and cloud feedbacks, and changes in the poleward transport of energy in the atmosphere and ocean (Goosse et al., 2018; Previdi et al., 2021). It is strongest in boreal winter. Climate models have been shown to be able to reproduce the observed temperature and mean sea

ice trends in the Arctic, albeit with demonstrated discrepancies in other variables (Notz & SIMIP Community, 2020; Previdi et al., 2021).

Previous modelling studies have projected a decrease in the likelihood and duration of cold extremes at the high latitudes and over central and eastern North Ameria, but not over central Asia, due to future Arctic sea-ice loss (Screen et al., 2015a, 2015b). Another study has projected no change in the frequency or duration of cold weather outbreaks but a decrease in their severity in the US, Europe and East Asia (Ayarzagüena & Screen, 2016).

By contrast, winter warm extremes in relation to Arctic changes are much less studied. Increasingly for the Arctic region, however, mild winter conditions are becoming a concern because short-lived warm spells in winter are associated with rain on snow events. These events have wide-ranging impacts on vegetation, soil organisms, Arctic species, and human livelihoods, and they are projected to become more frequent in future (Serreze et al., 2021). Novel work is needed to investigate changes in winter warm extremes due to future Arctic sea-ice loss.

Furthermore, there is uncertainty about the influence of Arctic amplification on atmospheric circulation and mid-latitude severe weather (Cohen et al., 2020; Overland et al., 2021). For example, coupled atmosphere-ocean models suggest that Arctic sea-ice loss intensifies the wintertime Siberian High, but the temperature reponse is not robustly simulated (Labe et al., 2020; Screen et al., 2018; Screen & Blackport, 2019). Uncertainty comes from the different climate models, different forcings and methodologies, and in some cases, relatively small ensembles used (Cohen et al., 2020; Overland et al., 2016; Smith et al., 2019). This provides a strong rationale for using coordinated experiments in a large multi-model ensemble.

The Polar Amplification Model Intercomparison Project (PAMIP) provides a set of coordinated experiments designed to understand the causes as well as the consequences of polar amplification (Smith et al., 2019). It is a contribution to the Coupled Model Intercomparison Project Phase 6 (CMIP6) (Eyring et al., 2016). By running standardized experiments in different climate models and generating large ensembles from each model, PAMIP helps to provide a better estimate of the forced response and to quantify model uncertainty (Screen et al., 2018). PAMIP simulations have been used to study, for instance, the effects of Arctic sea-ice loss and/or warming on the North Pacific jet stream (Ronalds et al., 2020), poleward heat transport (Audette et al., 2021), the wintertime Siberian High (Labe et al., 2020), and mid-latitude westerly winds (Smith et al., 2022).

Here, we utilize the atmosphere-only PAMIP experiments for the first time to assess the respective responses of boreal winter cold and warm extremes to future Arctic sea-ice loss and sea surface temperature (SST) change associated with 2°C global mean warming above pre-industrial levels. We focus on land regions in the Northern Hemisphere, where extreme temperatures have direct impacts on their communities. Using daily temperature output from ten PAMIP models, each of which having up to 200 ensemble members, we examine the changes in 1-in-20-year cold and warm events. Expanding on previous studies, we study both cold and hot extremes and also examine the respective responses to sea-ice loss and SST change.

Consdirtation of the response to SST change is important, as the local cooling in response to sea-ice loss proposed in earlier studies may be overwhelmed by warming due to global SST change.

2 Data and Methods

2.1 PAMIP experiments

We compare model-simulated temperatures between three PAMIP atmosphere-only time slice experiments. First, we use an experiment forced by present-day (i.e., 1979-2008 climatological) SSTs and sea-ice concentration (Smith et al., 2019), denoted as 'pd' hereafter. Second, we use an experiment forced by present-day SSTs but future Arctic sea-ice concentration representative of 2°C global average warming above pre-industrial levels. This experiment is denoted as 'futArcSIC'. Third, we make use of an experiment in which climate models are forced by future SSTs representative of 2°C global warming but sea-ice concentration at the present-day level. This experiment is referred to as 'futSST'. We note that 2°C global average warming above pre-industrial levels is equivalent to 15.7°C in absolute global mean temperature, and that sea ice thickness changes are not included this these experiments (Smith et al., 2019). All of these experiments are one-year time slices with radiative forcing from the year 2000. As such, comparing futArcSIC with pd provides an estimate of extreme temperature changes due to future Arctic sea-ice concentration loss, whereas comparing futSST with pd provides an estimate of changes due to future SST change.

These experiments are run by climate models with a minimum of ~100 winters to generate large ensembles that are suitable for studying climate extremes (Smith et al., 2019). We make use of daily minimum (tasmin) and maximum (tasmax) near-surface air temperature outputs from ten climate models, as listed in supplementary Table S1. Specifically, we focus on the respective changes in minimum tasmin and maximum tasmax in boreal winter (December-January-February, or DJF) due to future Arctic sea-ice loss and SST change. All included models have daily tasmin and tasmax outputs for pd and futArcSIC. A subset of six models also have outputs for futSST. More than half of the models have at least 200 ensemble members. We use a maximum of 200 members from each model to compute the differences in 1-in-20-year winter minimum and maximum temperatures at each model grid point due to Arctic sea-ice loss and SST change. A 1-in-20-year event has a 5% chance of occurring in any given year, and we use it to represent extremes. A maximum of 200 members is a large enough sample size for this return period, but more members could have been used from some models (Table 1) (Thompson et al., 2017). By focusing on DJF minimum and maximum temperatures, we avoid averaging out the extremes in seasonal means (Francis, 2021). We conduct an additional return period analysis at the regional scale (Sections 2.2 and 2.3).

The included models have different atmospheric horizontal resolutions, ranging from 0.83° x 0.56° in HadGEM3-GC31-MM (Andrews et al., 2020) to ~2.8° in CanESM5 (Swart et al., 2019). For all grid cells in the Northern Hemisphere, we calculate the difference in 1-in-20-year minimum and maximum temperatures between the PAMIP experiments in individual models, as well as the multi-model mean difference (giving each model equal weight). When considering the individual models, we compute the temperature difference in the models' native grids. When

considering the multi-model mean, we regrid (through nearest-neighbour regridding) all model results to CanESM5's grid because it is the coarsest among the studied models, before computing the multi-model mean difference.

2.2 Regions

We perform analyses in 14 selected regions in the northern mid to high latitudes. These regions are selected from a pre-defined set of regions that are ~2 Mm^2 in size and designed for examining climate extremes and their impacts (Stone, 2019). The regions are shown in Figure S1.

2.3 Return period analyses

We compute return periods by sorting each temperature series of DJF minimum tasmin (and maximum tasmax) in ascending (descending) order and dividing the length of the series by the ranks of the temperature values within the sorted series. We find the difference in 1-in-20-year temperature between experiments at each model grid point. We test whether the two samples of temperatures (i.e., not just the 1-in-20-year values) from different experiments are significantly different using a Kolmogorov-Smirnov (KS) test (Daniel, 1990).

For the regional analysis, we produce and compare return period curves from the pd simulations and the ERA5 reanalysis (Hersbach et al., 2020). We find the regional mean DJF minimum tasmin and maximum tasmax by area-weighted averaging values across native grid cells whose grid point values are within the boundary of each region. Since the present-day conditions in pd are based on 1979-2008 climatology, we extract ERA5 data from the same time period for comparison. This comparison is not completely like-for-like because inter-annual variability exists in ERA5 but not in pd, which has constant boundary forcing. To remove the climate change signal from the regional ERA5 time series and approximately isolate internal variability, we fit a linear trend to the corresponding DJF mean tasmin (and tasmax) time series and remove this trend from the 1979-2008 DJF minimum tasmin (maximum tasmax) time series. This ensures that the trends in the winter season, not just in the extremes, are removed. We then add the regional 1995-2005 average DJF minimum tasmin (maximum tasmax) value in ERA5 to the detrended data, to obtain absolute temperatures for comparison with model output . We choose the 1995-2005 decade because it is centred on year 2000, the year from which radiative forcing is used in the PAMIP time slice experiments.

The modelled pd data do not need detrending because they come from large ensembles of time slice simulations and use a constant radiative forcing. To bias-correct data from each model, we remove from each ensemble member the bias between ensemble-mean regional-mean DJF minimum tasmin (maximum tasmax) and the corresponding 1979-2008 mean regional-mean

ERA5 value. We then find the return period curves based on bias-corrected pd data and detrended ERA5 data.

We estimate the uncertainty associated with the ERA5 return period curve by resampling the ERA5 distribution 1000 times, though acknowledging that uncertainty sampling in the extremes is limited by the observations. The comparison between individual model return period curves and the ERA5 90% confidence interval enables us to identify models that simulate present-day winter temperature extremes reasonably well in the selected regions. Figures 1a and 1c show this comparison for North EEA, for which four and two models (indicated by dotted lines) are excluded in model selection for cold and warm extremes, respectively, because their return period curves are outside the ERA5 envelope at a majority of return periods.

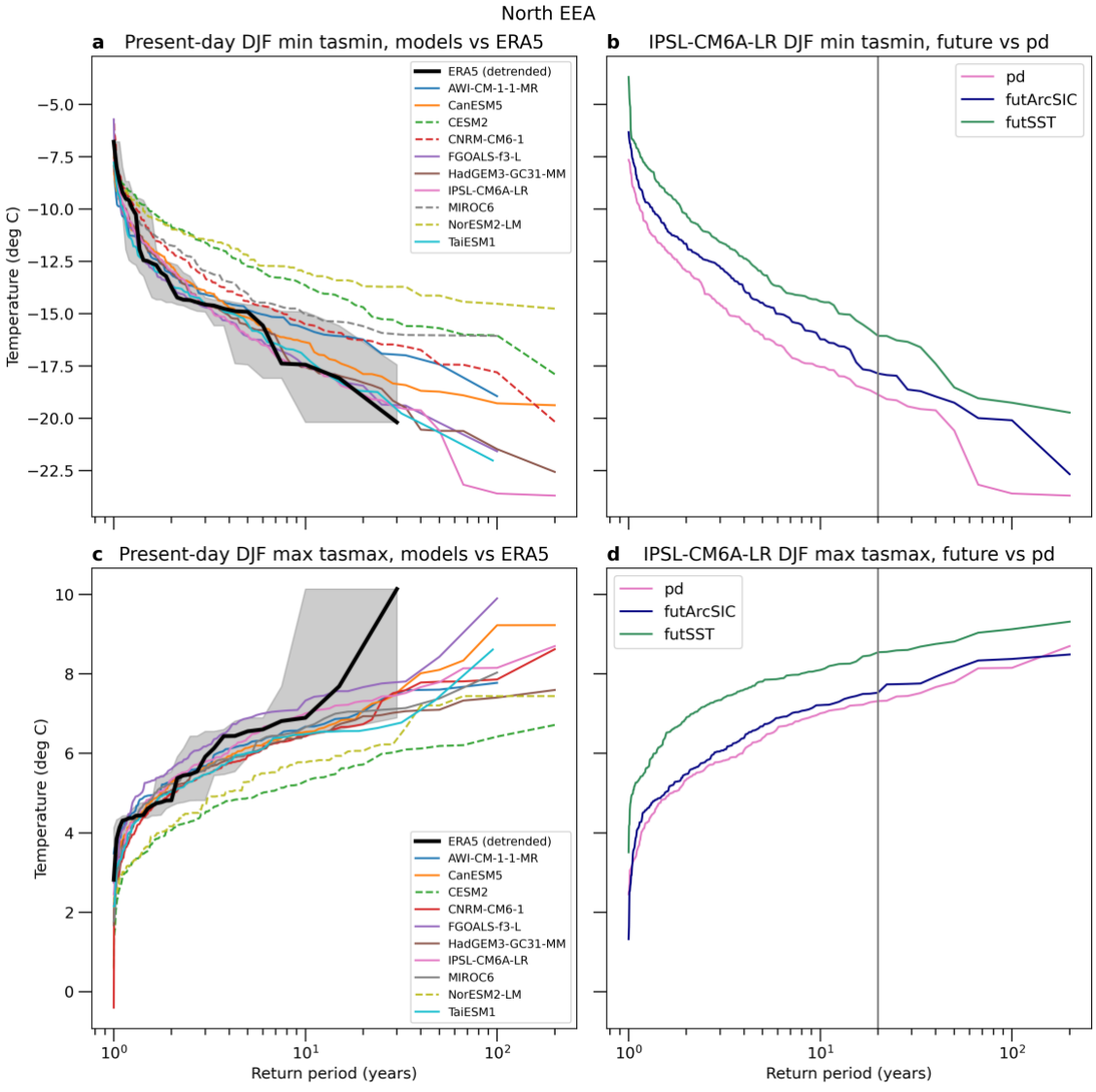

Figure 1. Return period curves for North EEA. (a) The comparison between present-day bias-corrected DJF minimum daily minimum temperature data from individual climate models (colored lines) and detrended ERA5 over the period 1979-2008 (thick black line). The grey

envelope shows the 90% uncertainty associated with the ERA5 curve found by bootstrapping. Solid colored lines indicate models that are included because they largely fall within the ERA5 envelope, whereas dashed colored lines indicate excluded models. (b) Example results from the IPSL-CM6A-LR model only, showing DJF minimum daily minimum temperatures in the pd (pink line), futArcSIC (navy line) and futSST (green line) experiments. The grey vertical line indicates the 20-year return period. (c) Same as (a) but for DJF maximum of daily maximum temperature. (d) Same as (b) but for DJF maximum of daily maximum temperature.

To assess the effects of future Arctic sea-ice concentration loss and SST change on regional winter extremes, we find the return period curves using the futArcSIC and futSST ensembles, respectively. Example return period curves from futArcSIC, futSST and pd simulated by IPSL-CM6A-LR for the North EEA region are shown Figures 1b and 1d. For each model and region, we find the temperature difference between futArcSIC and pd, and between futSST and pd, at the 20-year return period. For analyses involving futArcSIC, we report the temperature differences from the individual models, as well as the multi-model mean across all 10 models and the mean across a subset of models that simulate the present day well (according to ERA5). This subset varies from region to region and between cold and warm extremes (Figure S2). For analyses involving futSST, we mainly report the multi-model mean temperature difference across the 6 models for which there is output for this experiment (Table S1) for brevity.

3 Results

3.1 Reponses to sea-ice loss

Figure 2a shows the multi-model-mean difference in 1-in-20-year winter cold extremes between futArcSIC and pd in the Northern Hemisphere. The largest warming, of over ~2.5°C, is projected for northern and eastern Canada near Hudson Bay. The futArcSIC and pd winter minimum temperature distributions are statistically significantly different at the 5% level, indicating amplified warming in boreal winter cold extremes due to future Arctic sea-ice loss, as global average temperature is 1.4°C higher in futArcSIC than in pd (Smith et al., 2019). A statistically significant warming of ~2°C is also projected for Alaska. These results are generally consistent across the models (Figure S3), likely due the close proximity to imposed sea ice reductions in Hudson Bay, Labrador Sea and Bering-Chukchi Seas (Smith et al., 2022).

In the multi-model mean, ~1°C warming is simulated in Greenland, across Scandanavia and in northern Russia. However, there is inconsistency in the sign between the models, with MIROC6 and TaiESM1 simulating some cooling in central Greenland, CanESM5 and CESM2 simulating cooling over Scandanavia, and four models simulating cooling in different parts of north Russia (Figure S3). At the mid and low latitudes, cooling responses are seen for the United States, parts of Europe and central and eastern Asia. In some models, this cooling is up to about -1°C, suggesting intensified winter cold extremes. However, this response is not statistically significant

and is less robust in terms of spatial extent and magnitude than the aforementioned higher-latitude warming response (Figure S3).

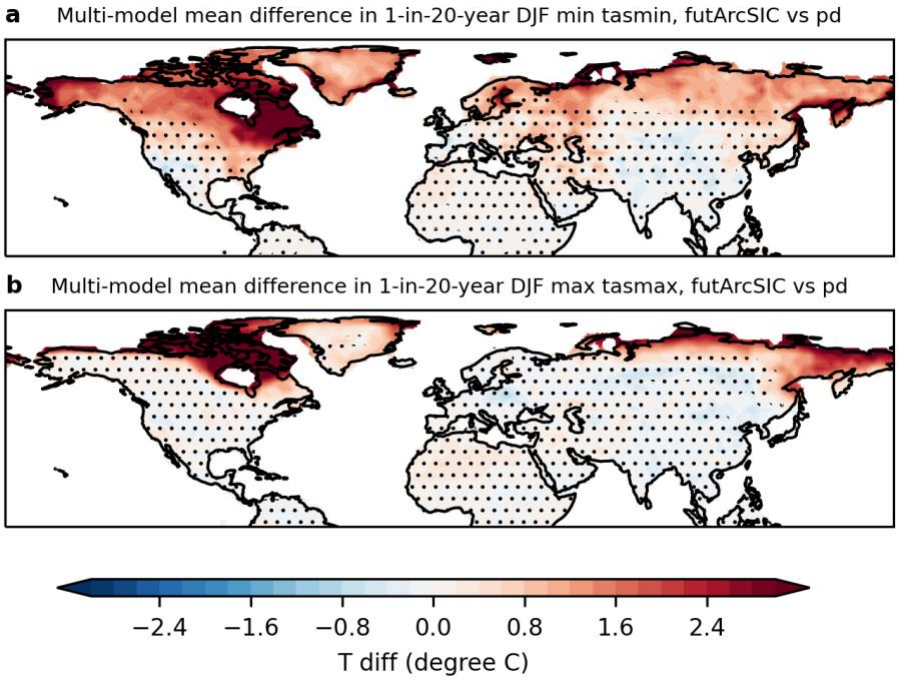

Figure 2. Changes in 1-in-20-year (a) DJF minimum of daily minimum temperature and (b) DJF maximum of daily maximum temperature in the Northern Hemisphere due to future Arctic sea-ice loss. The panels show the multi-model mean across ten PAMIP models. Stippling indicates where the temperature distributions from futArcSIC and pd are not statistically significantly different at the 5% level, based on a KS test.

Figure 2b shows the multi-model-mean difference in 1-in-20-year winter warm extremes between futArcSIC and pd. Statistically significant changes are only simulated in the high latitudes, with northern Canada showing the strongest warming, of over ~2.5°C, followed by northeastern Russia (~2°C). These changes are generally consistent across the models (Figure S4). The multi-model-mean indicates widespread cooling of up to - 0.4°C that is not statistically significant across most parts of North America, Eurasia and central Africa. Individual models simulate a stronger cooling response in different parts of the continents, although the responses are not statistically significant (Figure S4). A greater warming of cold extremes (Figures 2a and S3) compared to warm extremes (Figures 2b and S4) implies reduced temperature variance.

Next, we examine the regionally averaged differences in 1-in-20-year winter cold and warm extremes between futArcSIC and pd in 14 selected regions over the mid-to-high northern latitudes, where the largest and most significant temperature responses are simulated. Figure 3 shows the results from the individual models (circles), as well as the multi-model-mean responses across the 10 models (yellow crosses) and the multi-model-mean responses across

selected models (i.e., those that simulate regional present-day climates that are consistent with the ERA5 reanalysis; black squares).

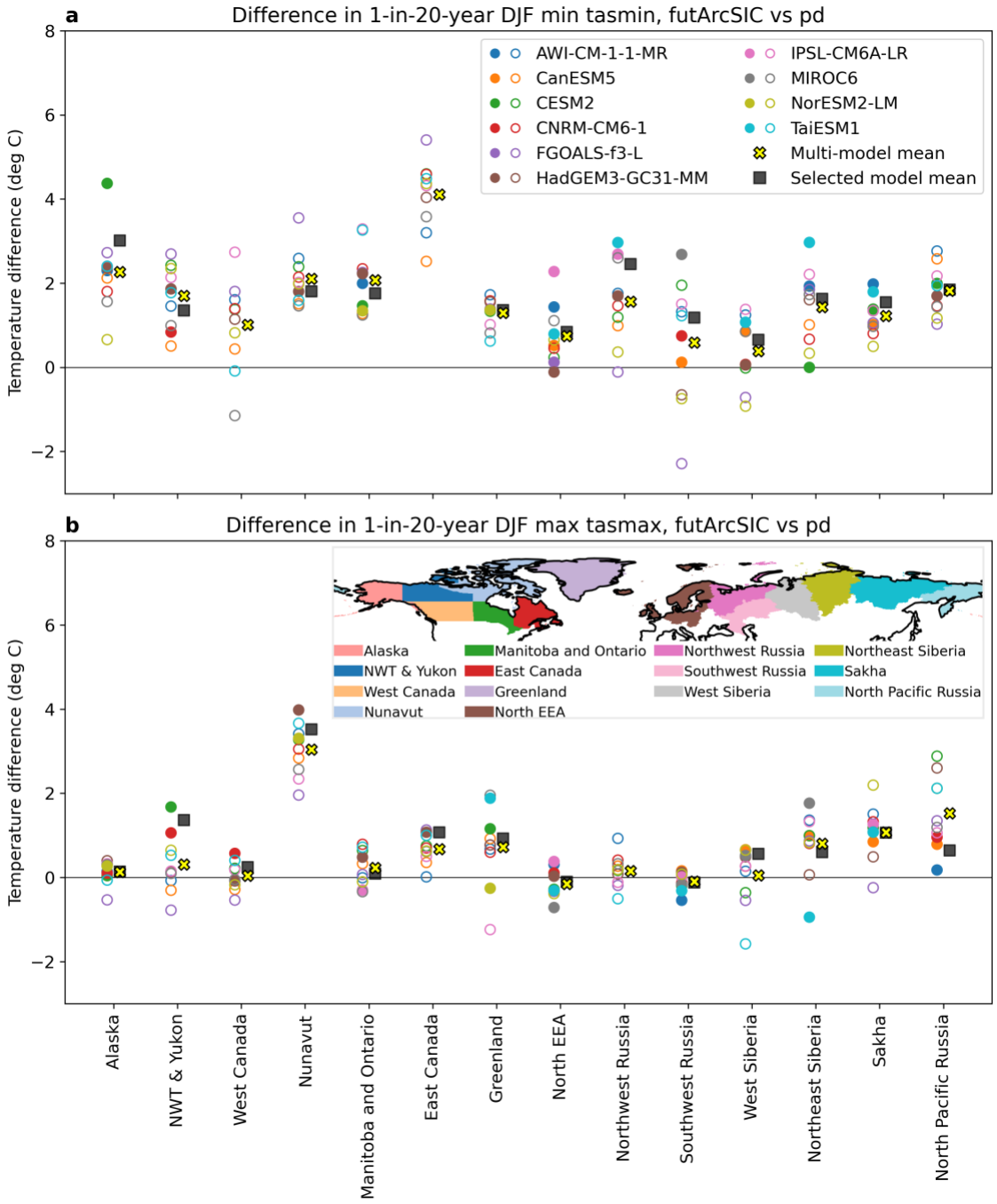

Figure 3. Temperature differences in (a) DJF minimum daily minimum temperature and (b) DJF maximum daily maximum temperature with a 20-year return period between futArcSIC and pd, in 14 chosen regions (locations of which are shown in the inset). Each circle represents one PAMIP model, with a filled circle indicating consistency between that model's corresponding bias-corrected pd return period curve and the equivalent ERA5 return period curve from 1979-

2008 for the region, and an empty circle indicating inconsistency with ERA5. Black squares show the mean across the selected models indicated by the filled circles. Yellow crosses show the mean across all ten models.

Like in Figure 2a, the regional analysis for cold extremes (Figure 3a) reveals the largest average warming response in East Canada, with the models simulating regional-mean warming between 2 and 6°C. In the multi-model mean, all selected regions are projected to experience a warming of winter cold extremes due to Arctic sea-ice loss, with values ranging from 0.4°C (inter-model range: -0.9 to 1.4°C) in West Siberia to 4.1°C (range: 2.5 to 5.4°C) in East Canada. The mean results are similar across the subsets of models (note, no model is consistent with ERA5 in East and West Canada even after mean bias correction). Despite the general warming response seen in the multi-model mean, some models simulate intensified winter cold extremes in regions including West Canada, North EEA, Northwest and Southwest Russia, and West and Northeast Siberia. However, these cooling responses are not statistically significant (Figure S3) and could be due to internal variability.

The regional results for winter warm extremes are shown in Figure 3b. Nunavut in northern Canada has the largest multi-model-mean warming response to future Arctic sea-ice loss, with individual models simulating 2 to 4°C warming. As shown in Figure 2b, North Pacific Russia has the second largest mean response at 1.5°C (range: 0.2 to 2.9°C). For the rest of the regions, the multi-model-mean response is within about +/- 1°C, ranging from -0.2°C (range: -0.7 to 0.4°C) in North EEA to 1.1°C (range: -0.2 to 2.2°C) in Sakha. Eleven of the 14 selected regions (except Nunavut, East Canada and North Pacific Russia) have at least one model simulating a cooling response, showing a smaller signal-to-noise ratio than cold extremes. Overall, Figure 3 shows that the pd model simulations do not compare very well with reanalysis even after bias correction, partially because of the idealized nature of the experiments. However, this does not affect our main results.

3.2 Responses to SST change

Figure 4a shows that warmer SSTs associated with 2°C global mean warming increase 1-in-20-year cold temperatures over land in the Northern Hemisphere in the multi-model mean. This warming is statistically significant at the 5% level. No cooling response is shown in the multi-model mean at any location. In general, individual models agree on a strong (~3°C) warming signal in North America, particularly in the western parts (Figure S5). The cold response in Eurasia to future SST change is more variable, with IPSL-CM6A-LR showing strong warming in

the northern parts, whereas FGOALS-f3-L shows cooling in those parts but relatively strong warming in east Asia (Figure S5). These differences may be affected by sampling variability.

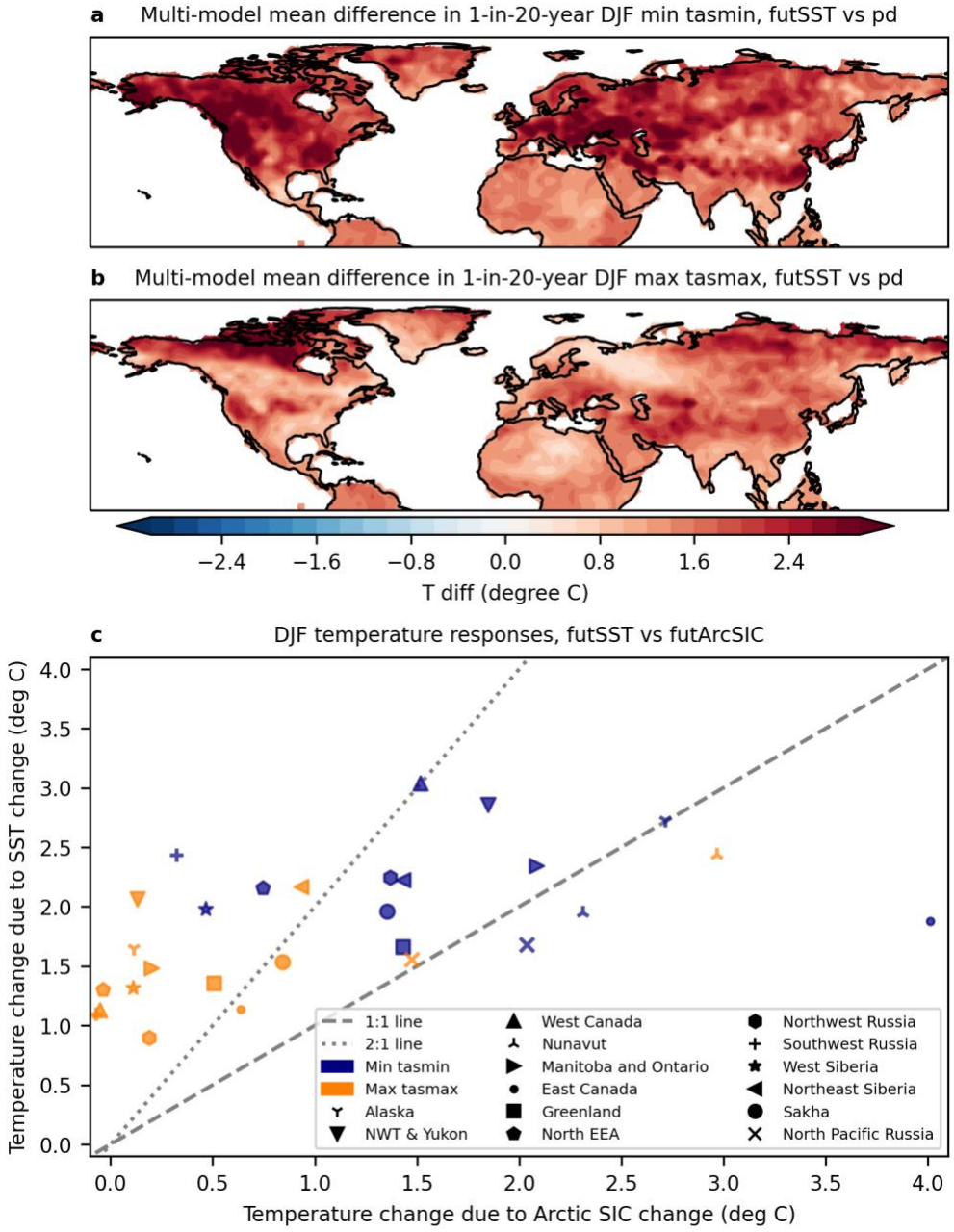

Figure 4. (a) Multi-model mean changes in 1-in-20-year DJF minimum of daily minimum temperature in the Northern Hemisphere due to future SST change. The temperature distributions from futSST and pd are statistically significantly different at the 5% level based on a KS test. (b) Same as (a) but for DJF maximum of daily maximum temperature. (c) Comparison between the multi-model mean temperature changes due to future Arctic sea-ice loss (x-axis) and the corresponding changes due to future SST change (y-axis). Navy points indicate changes in 1-in-20-year DJF minimum of daily minimum temperature, whereas orange points indicate changes in

1-in-20-year DJF maximum of daily maximum temperature. Each point represents the regional mean in one particular region. The dashed line indicates a 1:1 relationship, whereas the dotted line indicates a 2:1 relationship.

Future SST change is also projected to warm winter warm extremes significantly in all Northern Hemisphere land grid cells in the multi-model mean, as shown in Figure 4b. However, both the multi-model mean and individual model results (Figure S6) indicate that the warm extreme response is smaller compared to the cold extreme response in almost all places except northern Canada. Small inter-model differences are seen in the warm extreme response to SST change, with CanESM5 simulating cooling in Greenland and northeastern Russia that is not statistically significant, for example.

With previous evidence that responses to sea ice and greenhouse gas forcing are approximately linearly additive (McCusker et al., 2017), it may be reasonable to deduce the combined mean 1-in-20-year winter temperature responses to Arctic sea-ice loss and ocean warming from Figures 3 and 4. For cold extremes, even in places where Arctic sea-ice loss is simulated to intensify them (e.g., in southwestern United States, parts of Europe, central and eastern Asia, though not statistically significantly; Figure S3), warming due to SST change overwhelms this cooling effect, resulting in net warming (not shown).

Indeed, by comparing the multi-model mean of the 1-in-20-year cold temperature differences due to Arctic sea-ice change (x-axis) and SST change (y-axis) over the 14 selected regions in Figure 4c (navy markers), we find that the warming response to future SST change is larger than or equal to the response to future Arctic sea-ice loss in 11 regions (i.e., except Nunavut, East Canada and North Pacific Russia). The three exceptions suggest that the response to sea-ice loss is by far the largest near the regions of sea-ice loss, whereas warming due to SST change is more spatially homogeneous. The ratio of SST change-induced response to sea ice loss-induced response ranges from 0.5 in East Canada to 7.5 in Southwest Russia. Since all selected regions are projected to experience multi-model-mean warming to both sea-ice and SST changes, an enhanced combined response is expected. For East Canada, this may mean a combined response of 5.8°C.

For warm extremes, warming from SST change also dominates over the small and non-statistically significant Arctic sea ice-loss induced cooling responses in North America, Eurasia and Africa, resulting in net warming. Figure 4c shows this clearly, where all but one orange markers (i.e., except for Nuavut) are above the 1:1 identity line. The ratio of the magnitude of SST-induced response to the magnitude of sea ice-induced response ranges from 0.8 in Nunavut to 35 in North EEA (because of a near-zero response to sea ice). In Nunavut (northern Canada), where winter warm extreme is projected to become statistically significantly warmer due to Arctic sea-ice loss and SST change separately, the combined effect may mean intensification of

warm extremes by 5.4°C, although we emphasize that our results are based on idealized atmosphere-only experiments.

5 Discussion and Conclusions

Arctic amplification has been a topic of interest in the literature, not only because it is one of the strongest anthropogenic climate change signals, but also because of its wide-reaching effects on the climate system (Labe et al., 2020; Screen et al., 2013). This study is the first to use targeted and coordinated PAMIP experiments to examine the response of rare (1-in-20-year) winter temperature extremes to Arctic sea-ice loss and SST change at 2°C global mean warming above pre-industrial levels. It is also the first to investigate winter warm extremes, and to bias-correct the PAMIP simulations and apply model selection based on reanalysis data.

We have shown a multi-model-mean warming response of winter cold extremes to future Arctic sea-ice loss across the mid and high latitudes. This is consistent with the projected decrease in the likelihood and severity of mid- and high-latitude cold extremes in previous studies (Ayarzagüena & Screen, 2016; Screen et al., 2015b). For 8 of the 14 selected regions (excluding West Canada, North EEA, Northwest and Southwest Russia, and West and Northeast Siberia), the sign of change is robust across ten models. Where a local cooling response is simulated in some models, the location of this cooling is not robust across models, and may be a sign of internal variability. We cannot rule out a weak cooling response, as suggested by previous studies (Labe et al., 2020; Zappa et al., 2021), but it appears to be model dependent.

The winter cold extreme response to future SST change is more robust, with almost all of the Northern Hemisphere showing a warming response in all available models. Notably, this warming response exceeds the sea ice-induced cooling response in southwestern United States, western Europe, and central and eastern Asia. Overall, our results imply that some of the adverse impacts of cold extremes on, for instance, human health (Mäkinen, 2007; Vasconcelos et al., 2013) and transport and power supply (Screen et al., 2015b) are expected to be lessened in the mid and high latitudes in the future. However, we stress that Arctic warming and sea-ice loss are already impacting the Arctic communities (Moerlein & Carothers, 2012), whose lifestyles and livelihoods were adapted to cold weather through generations of lived knowledge.

For winter warm extremes, we have shown that statistically significant responses to future Arctic sea-ice loss are limited to the high latitudes, primarily to northern Canada and northeastern Russia. Non-significant responses are found for the rest of the hemisphere, and overall the warm extreme response is weaker than the cold response. This suggests a reduced winter temperature variance due to Arctic sea-ice loss, which is consistent with the literature (Blackport et al., 2021; Collow et al., 2019; Screen, 2014). SST-induced warming is larger than the sea ice-induced changes in most places.

Warming of winter warm extremes in the high latitudes due to Arctic sea-ice loss and ocean warming can increase the chances of rain on snow events. Notable events have already occured in Arctic Canada (Rennert et al., 2009) and Russia (Forbes et al., 2016), which led to declines in ungulate (e.g., reindeer and musk oxen) populations that persisted for years and herders losing

food security and transportation (Serreze et al., 2021). Our results suggest that these communities are at an increased risk of these impacts in a 2°C warmer world, compared to the present day.

Sea-ice loss does not happen in isolation, but considering it together with future ocean warming is not routinely done. Going forward, we recommend researchers place a stronger focus on the SST component or the net response. Moreover, the combined effect of Arctic sea-ice loss and SST change on winter temperature extremes has not been studied here. Potential non-linearities in their effects may mean that a combined future sea-ice and SST experiment in PAMIP is important. Future work should also quantify the resulting impacts on various aspects of society through coupled climate and impact modelling.

Aside from sea-ice concentration loss and SST change, PAMIP provides a range of experiments designed to investigate the impacts of sea-ice thickness changes and full ocean dynamics (Smith et al., 2019), which have not been studied here. Our estimates of the responses to sea-ice loss may be conservative because both ice thickness changes (Labe et al., 2018) and atmosphere-ocean coupling (Deser et al., 2015, 2016; Smith et al., 2017) have been suggested to strengthen the response. It is recommended that researchers fully exploit the PAMIP data to investigate the effects of these changes.

Acknowledgments

We thank Tim Woollings for providing feedback to this manuscript. This work was funded by the NERC grant ArctiCONNECT (grant ID: NE/V005855/1). PAGW was supported by a NERC Independent Research Fellowship (grant no. NE/S014713/1). The authors have no conflicts of interests.

Availability Statement

The PAMIP data used in this study are available at Earth System Grid Federation (ESGF) via https://esgf-node.llnl.gov/search/cmip6/. A user guide for creating an ESGF account and downloading the data can be found at https://esgf.github.io/esgf-user-support/. PAMIP data information from each modeling center, including their contact information, can be found at https://www.cesm.ucar.edu/projects/CMIP6/PAMIP/. The ERA5 reanalysis data are available from the Copernicus Climate Data Store https://cds.climate.copernicus.eu/cdsapp#!/dataset/reanalysis-era5-single-levels?tab=overview.

References

Andrews, M. B., Ridley, J. K., Wood, R. A., Andrews, T., Blockley, E. W., Booth, B., et al. (2020). Historical Simulations With HadGEM3-GC3.1 for CMIP6. *Journal of Advances in Modeling Earth Systems, 12*(6), 1–34. https://doi.org/10.1029/2019MS001995

Audette, A., Fajber, R. A., Kushner, P. J., Wu, Y., Peings, Y., Magnusdottir, G., et al. (2021). Opposite Responses of the Dry and Moist Eddy Heat Transport Into the Arctic in the

PAMIP Experiments. *Geophysical Research Letters*, *48*(9), 1–10. https://doi.org/10.1029/2020GL089990

Ayarzagüena, B., & Screen, J. A. (2016). Future Arctic sea ice loss reduces severity of cold air outbreaks in midlatitudes. *Geophysical Research Letters*, *43*(6), 2801–2809. https://doi.org/10.1002/2016GL068092

Blackport, R., Fyfe, J. C., & Screen, J. A. (2021). Decreasing subseasonal temperature variability in the northern extratropics attributed to human influence. *Nature Geoscience*, *14*(10), 719–723. https://doi.org/10.1038/s41561-021-00826-w

Cohen, J., Zhang, X., Francis, J., Jung, T., Kwok, R., Overland, J., et al. (2020). Divergent consensuses on Arctic amplification influence on midlatitude severe winter weather. *Nature Climate Change*, *10*(1), 20–29. https://doi.org/10.1038/s41558-019-0662-y

Collow, T. W., Wang, W., & Kumar, A. (2019). Reduction in northern midlatitude 2-m temperature variability due to Arctic sea ice loss. *Journal of Climate*, *32*(16), 5021–5035. https://doi.org/10.1175/JCLI-D-18-0692.1

Daniel, W. W. (1990). *Applied Nonparametric Statistics* (2nd ed.). PWS-KENT Pub.

Deser, C., Tomas, R. A., & Sun, L. (2015). The role of ocean-atmosphere coupling in the zonal-mean atmospheric response to Arctic sea ice loss. *Journal of Climate*, *28*(6), 2168–2186. https://doi.org/10.1175/JCLI-D-14-00325.1

Deser, C., Sun, L., Tomas, R. A., & Screen, J. (2016). Does ocean coupling matter for the northern extratropical response to projected Arctic sea ice loss? *Geophysical Research Letters*, *43*(5), 2149–2157. https://doi.org/10.1002/2016GL067792

Eyring, V., Bony, S., Meehl, G. A., Senior, C. A., Stevens, B., Stouffer, R. J., & Taylor, K. E. (2016). Overview of the Coupled Model Intercomparison Project Phase 6 (CMIP6) experimental design and organization. *Geoscientific Model Development*, *9*(5), 1937–1958. https://doi.org/10.5194/gmd-9-1937-2016

Forbes, B. C., Kumpula, T., Meschtyb, N., Laptander, R., MacIas-Fauria, M., Zetterberg, P., et al. (2016). Sea ice, rain-on-snow and tundra reindeer nomadism in Arctic Russia. *Biology Letters*, *12*(11), 4–8. https://doi.org/10.1098/rsbl.2016.0466

Francis, J. A. (2021). RE: Article misidentifies study as “landmark.” Retrieved November 29, 2022, from https://www.science.org/do/10.1126/comment.763356/full/

Francis, J. A., & Wu, B. (2020). Why has no new record-minimum Arctic sea-ice extent occurred since September 2012? *Environmental Research Letters*, *15*(11). https://doi.org/10.1088/1748-9326/abc047

Goosse, H., Kay, J. E., Armour, K. C., Bodas-Salcedo, A., Chepfer, H., Docquier, D., et al. (2018). Quantifying climate feedbacks in polar regions. *Nature Communications*, *9*(1). https://doi.org/10.1038/s41467-018-04173-0

Hersbach, H., Bell, B., Berrisford, P., Hirahara, S., Horányi, A., Muñoz-Sabater, J., et al. (2020). The ERA5 global reanalysis. *Quarterly Journal of the Royal Meteorological Society*, (March), 1–51. https://doi.org/10.1002/qj.3803

Labe, Z., Peings, Y., & Magnusdottir, G. (2018). Contributions of Ice Thickness to the Atmospheric Response From Projected Arctic Sea Ice Loss. *Geophysical Research Letters*, *45*(11), 5635–5642. https://doi.org/10.1029/2018GL078158

Labe, Z., Peings, Y., & Magnusdottir, G. (2020). Warm Arctic, Cold Siberia Pattern: Role of Full Arctic Amplification Versus Sea Ice Loss Alone. *Geophysical Research Letters*, *47*(17), 1–11. https://doi.org/10.1029/2020GL088583

Mäkinen, T. M. (2007). Human cold exposure, adaptation, and performance in high latitude environments. *American Journal of Human Biology*, *19*(2), 155–164. https://doi.org/10.1002/ajhb.20627

McCusker, K. E., Kushner, P. J., Fyfe, J. C., Sigmond, M., Kharin, V. V., & Bitz, C. M. (2017). Remarkable separability of circulation response to Arctic sea ice loss and greenhouse gas forcing. *Geophysical Research Letters*, *44*(15), 7955–7964. https://doi.org/10.1002/2017GL074327

Moerlein, K. J., & Carothers, C. (2012). Total Environment of Change: Impacts of Climate Change and Social Transitions on Subsistence Fisheries in Northwest Alaska. *Ecology and Society*, *17*(1). https://doi.org/10.5751/es-04543-170110

Notz, D., & SIMIP Community. (2020). Arctic Sea Ice in CMIP6. *Geophysical Research Letters*, *47*(10), 1–11. https://doi.org/10.1029/2019GL086749

Overland, J. E., Dethloff, K., Francis, J. A., Hall, R. J., Hanna, E., Kim, S. J., et al. (2016). Nonlinear response of mid-latitude weather to the changing Arctic. *Nature Climate Change*, *6*(11), 992–999. https://doi.org/10.1038/nclimate3121

Overland, J. E., Ballinger, T. J., Cohen, J., Francis, J. A., Hanna, E., Jaiser, R., et al. (2021). How do intermittency and simultaneous processes obfuscate the Arctic influence on midlatitude winter extreme weather events? *Environmental Research Letters*, *16*(4). https://doi.org/10.1088/1748-9326/abdb5d

Previdi, M., Smith, K. L., & Polvani, L. M. (2021). Arctic amplification of climate change: a review of underlying mechanisms. *Environmental Research Letters*, *16*(9), 093003. https://doi.org/10.1088/1748-9326/ac1c29

Rantanen, M., Karpechko, A. Y., Lipponen, A., Nordling, K., Hyvärinen, O., Ruosteenoja, K., et al. (2022). The Arctic has warmed nearly four times faster than the globe since 1979. *Communications Earth & Environment*, *3*(168), 1–10. https://doi.org/10.1038/s43247-022-00498-3

Rennert, K. J., Roe, G., Putkonen, J., & Bitz, C. M. (2009). Soil thermal and ecological impacts of rain on snow events in the circumpolar arctic. *Journal of Climate*, *22*(9), 2302–2315.

https://doi.org/10.1175/2008JCLI2117.1

Ronalds, B., Barnes, E. A., Eade, R., Peings, Y., & Sigmond, M. (2020). North Pacific zonal wind response to sea ice loss in the Polar Amplification Model Intercomparison Project and its downstream implications. *Climate Dynamics*, *55*(7–8), 1779–1792. https://doi.org/10.1007/s00382-020-05352-w

Screen, J. A. (2014). Arctic amplification decreases temperature variance in northern mid- to high-latitudes. *Nature Climate Change*, *4*(7), 577–582. https://doi.org/10.1038/nclimate2268

Screen, J. A., & Blackport, R. (2019). How Robust is the Atmospheric Response to Projected Arctic Sea Ice Loss Across Climate Models? *Geophysical Research Letters*, *46*(20), 11406–11415. https://doi.org/10.1029/2019GL084936

Screen, J. A., Simmonds, I., Deser, C., & Tomas, R. (2013). The atmospheric response to three decades of observed arctic sea ice loss. *Journal of Climate*, *26*(4), 1230–1248. https://doi.org/10.1175/JCLI-D-12-00063.1

Screen, J. A., Deser, C., & Sun, L. (2015a). Projected changes in regional climate extremes arising from Arctic sea ice loss. *Environmental Research Letters*, *10*(8). https://doi.org/10.1088/1748-9326/10/8/084006

Screen, J. A., Deser, C., & Sun, L. (2015b). Reduced risk of North American cold extremes due to continued arctic sea ice loss. *Bulletin of the American Meteorological Society*, *96*(9), 1489–1503. https://doi.org/10.1175/BAMS-D-14-00185.1

Screen, J. A., Deser, C., Smith, D. M., Zhang, X., Blackport, R., Kushner, P. J., et al. (2018). Consistency and discrepancy in the atmospheric response to Arctic sea-ice loss across climate models. *Nature Geoscience*, *11*(3), 155–163. https://doi.org/10.1038/s41561-018-0059-y

Serreze, M. C., Gustafson, J., Barrett, A. P., Druckenmiller, M. L., Fox, S., Voveris, J., et al. (2021). Arctic rain on snow events: Bridging observations to understand environmental and livelihood impacts. *Environmental Research Letters*, *16*(10). https://doi.org/10.1088/1748-9326/ac269b

Smith, D. M., Dunstone, N. J., Scaife, A. A., Fiedler, E. K., Copsey, D., & Hardiman, S. C. (2017). Atmospheric response to Arctic and Antarctic sea ice: The importance of ocean-atmosphere coupling and the background state. *Journal of Climate*, *30*(12), 4547–4565. https://doi.org/10.1175/JCLI-D-16-0564.1

Smith, D. M., Screen, J. A., Deser, C., Cohen, J., Fyfe, J. C., García-Serrano, J., et al. (2019). The Polar Amplification Model Intercomparison Project (PAMIP) contribution to CMIP6: investigating the causes and consequences of polar amplification. *Geoscientific Model Development Discussions*, *12*, 1139–1164. https://doi.org/10.5194/gmd-12-1139-2019

Smith, D. M., Eade, R., Andrews, M. B., Ayres, H., Clark, A., Chripko, S., et al. (2022). Robust

but weak winter atmospheric circulation response to future Arctic sea ice loss. *Nature Communications*, *13*(1), 1–15. https://doi.org/10.1038/s41467-022-28283-y

Stone, D. A. (2019). A hierarchical collection of political/economic regions for analysis of climate extremes. *Climatic Change*, *155*(4), 639–656. https://doi.org/10.1007/s10584-019-02479-6

Swart, N. C., Cole, J. N. S., Kharin, V. V., Lazare, M., Scinocca, J. F., Gillett, N. P., et al. (2019). The Canadian Earth System Model version 5 (CanESM5.0.3). *Geoscientific Model Development*, *12*(11), 4823–4873. https://doi.org/10.5194/gmd-12-4823-2019

Thompson, V., Dunstone, N. J., Scaife, A. A., Smith, D. M., Slingo, J. M., Brown, S., & Belcher, S. E. (2017). High risk of unprecedented UK rainfall in the current climate. *Nature Communications*, *8*(1), 1–6. https://doi.org/10.1038/s41467-017-00275-3

Vasconcelos, J., Freire, E., Almendra, R., Silva, G. L., & Santana, P. (2013). The impact of winter cold weather on acute myocardial infarctions in Portugal. *Environmental Pollution*, *183*, 14–18. https://doi.org/10.1016/j.envpol.2013.01.037

Zappa, G., Ceppi, P., & Shepherd, T. G. (2021). Eurasian cooling in response to Arctic sea-ice loss is not proved by maximum covariance analysis. *Nature Climate Change*, *11*(2), 106–108. https://doi.org/10.1038/s41558-020-00982-8

References from Supplementary Materials

Andrews, M. B., Ridley, J. K., Wood, R. A., Andrews, T., Blockley, E. W., Booth, B., et al. (2020). Historical Simulations With HadGEM3-GC3.1 for CMIP6. *Journal of Advances in Modeling Earth Systems*, *12*(6), 1–34. https://doi.org/10.1029/2019MS001995

Boucher, O., Servonnat, J., Albright, A. L., Aumont, O., Balkanski, Y., Bastrikov, V., et al. (2020). Presentation and Evaluation of the IPSL-CM6A-LR Climate Model. *Journal of Advances in Modeling Earth Systems*, *12*(7), 1–52. https://doi.org/10.1029/2019MS002010

Danabasoglu, G., Lamarque, J. F., Bacmeister, J., Bailey, D. A., DuVivier, A. K., Edwards, J., et al. (2020). The Community Earth System Model Version 2 (CESM2). *Journal of Advances in Modeling Earth Systems*, *12*(2), 1–35. https://doi.org/10.1029/2019MS001916

He, B., Bao, Q., Wang, X., Zhou, L., Wu, X., Liu, Y., et al. (2019). CAS FGOALS-f3-L Model Datasets for CMIP6 Historical Atmospheric Model Intercomparison Project Simulation. *Advances in Atmospheric Sciences*, *36*(8), 771–778. https://doi.org/10.1007/s00376-019-9027-8

Seland, Ø., Bentsen, M., Seland Graff, L., Olivié, D., Toniazzo, T., Gjermundsen, A., et al. (2020). The Norwegian Earth System Model, NorESM2 – Evaluation of theCMIP6 DECK and historical simulations. *Geoscientific Model Development Discussions*, (February), 1–68. https://doi.org/10.5194/gmd-2019-378

Semmler, T., Danilov, S., Gierz, P., Goessling, H. F., Hegewald, J., Hinrichs, C., et al. (2020).

562 Simulations for CMIP6 With the AWI Climate Model AWI-CM-1-1. *Journal of Advances*
563 *in Modeling Earth Systems*, *12*(9), 1–34. https://doi.org/10.1029/2019MS002009

564 Swart, N. C., Cole, J. N. S., Kharin, V. V., Lazare, M., Scinocca, J. F., Gillett, N. P., et al.
565 (2019). The Canadian Earth System Model version 5 (CanESM5.0.3). *Geoscientific Model*
566 *Development*, *12*(11), 4823–4873. https://doi.org/10.5194/gmd-12-4823-2019

567 Tatebe, H., Ogura, T., Nitta, T., Komuro, Y., Ogochi, K., Takemura, T., et al. (2019).
568 Description and basic evaluation of simulated mean state, internal variability, and climate
569 sensitivity in MIROC6. *Geoscientific Model Development*, *12*(7), 2727–2765.
570 https://doi.org/10.5194/gmd-12-2727-2019

571 Voldoire, A., Saint-Martin, D., Sénési, S., Decharme, B., Alias, A., Chevallier, M., et al. (2019).
572 Evaluation of CMIP6 DECK Experiments With CNRM-CM6-1. *Journal of Advances in*
573 *Modeling Earth Systems*. https://doi.org/10.1029/2019MS001683

574 Wang, Y. C., Hsu, H. H., Chen, C. A., Tseng, W. L., Hsu, P. C., Lin, C. W., et al. (2021).
575 Performance of the Taiwan Earth System Model in Simulating Climate Variability
576 Compared With Observations and CMIP6 Model Simulations. *Journal of Advances in*
577 *Modeling Earth Systems*, *13*(7), 1–28. https://doi.org/10.1029/2020MS002353